

Surface Fermi Contours and Phonon Anomalies in a Random Alloy

Michio Okada

*Department of Chemistry, Graduate School of Science, Osaka University,
1-1 Machikaneyama-cho, Toyonaka, Osaka 560-0043, Japan*

Eli Rotenberg

Advanced Light Source, Lawrence Berkeley National Laboratory, Berkeley, California 94720, USA

S.D. Kevan

Department of Physics, University of Oregon, Eugene, Oregon 94703, USA

J. Schäfer

Institut für Physik, Universität Augsburg, 86135 Augsburg, Bavaria, Germany

E.W. Plummer

*Department of Physics and Astronomy, University of Tennessee, Knoxville, TN 37996, USA and Solid State
Division, Oak Ridge National Laboratory, Oak Ridge, TN 37831-6057, USA*

The impact of compositional disorder on manybody couplings is a subject of prime focus in many materials systems. In this paper, we report photoemission measurements of $\text{Mo}_{1-x}\text{Re}_x(110)-(1\times 1)\text{H}$ alloy surfaces to probe the relationship between the surface Fermi contours and recently observed giant Kohn anomalies in the surface phonon dispersion relations. While our measured nesting vectors precisely predict the composition dependence of the anomalous wave vector, the widths of the Fermi contours cannot explain the rapid increase of the width of the anomaly with rhenium concentration. We conclude that the compositional disorder scatters the phonons much more strongly than the electrons even though these two manifolds remain strongly coupled.

The impact of compositional disorder on material properties is a subject of prime focus in many materials systems, ranging from simple metal alloys to complex oxides and compound semiconductors. The macroscopic properties of interest are driven microscopically by manybody couplings between the electron gas and various low-energy bosonic degrees of freedom. Disorder will broaden electronic and the bosonic modes to varying degrees, and in the limit of very strong damping, one or more of these modes can even become localized. The question of how the variously damped modes remain coupled is of enduring fundamental interest and also of much practical importance.

In this paper, we report photoemission measurements of $\text{Mo}_{1-x}\text{Re}_x(110)-(1\times 1)\text{H}$ alloy surfaces to probe the relationship between the surface Fermi contours and recently observed giant Kohn anomalies in the surface phonon dispersion relations.¹ These anomalies are interesting because both the position and the width of the anomaly vary systematically as a function of composition. Our measured nesting vectors predict the composition dependence of the anomalous wave vector with good precision. However, the widths of the Fermi contours cannot explain the observed rapid increase of the width of the anomaly with rhenium concentration. In k -space, the electron states remain sharp while the phonon anomaly broadens by more than an order of magnitude. We conclude that the compositional disorder scatters the phonons much more strongly than the electrons even though these two manifolds remain strongly coupled.

The hydrogen-saturated $\text{Mo}_{1-x}\text{Re}_x(110)$ alloy surfaces offer ideal systems to measure how evolution of a microscopic observable – the Fermi surface – impacts surface lattice dynamical properties. The parent system $\text{Mo}(110)$ exhibits a dramatically deep and sharp anomaly in the phonon dispersion curves measured by inelastic helium atom scattering (HAS).^{2,3} Recent first principles density-functional theory calculations⁴⁻⁷ as well as angle-resolved photoemission measurements of the surface Fermi contours for this system⁸ and closely-related $\text{W}(110)-(1\times 1)\text{H}$ ^{9,10} have provided strong evidence that these observations can be attributed a giant Kohn anomaly.¹¹ These anomalies are driven by nesting between segments of the surface Fermi contours, leading to enhanced coupling between surface phonons and low-energy excitations in the electron-hole pair continuum. Moreover, the $\text{Mo}_{1-x}\text{Re}_x$ system has been shown to follow the rigid band paradigm,¹² at least for states near the Fermi level that drive the Kohn anomaly,¹³ so that the Fermi surface can be tuned by

varying the alloy composition. Recent HAS measurements indicate that the wave vector of the phonon anomaly shifts smoothly in $\text{Mo}_{1-x}\text{Re}_x(110)$ as a function of alloy composition.¹

In this paper, we focus on the position and width of the surface state Fermi contours as a function of alloy composition and relate these results to the position and width of the observed phonon anomaly. Our angle-resolved photoemission measurements show systematic changes in the surface state Fermi contours with increasing alloy concentration. The measured nesting vectors are in excellent agreement with the position of the measured phonon anomalies.¹ However, the width of the observed anomaly increases much more rapidly than predicted by the widths of our Fermi contours. We interpret this mismatch to indicate that the alloy positional disorder scatters the phonons much more strongly than the electrons. This prototypical system thereby demonstrates the potential for continuous Fermi-surface tuning with randomly alloying as a tool for controlling the surface and interfacial properties.

ARUPS experiments were performed at beamline 7.0 of the Advanced Light Source at a photon energy of 100 eV. The base pressure of the ARUPS chamber was 8×10^{-11} Torr. The combined monochromator and energy analyzer energy resolution was ~ 80 meV, and the momentum resolution was a few percent of the width of the Brillouin zone. $\text{Mo}_{1-x}\text{Re}_x(110)$ ingots with $x = 0.00, 0.05, 0.15$, and 0.25 were grown by the crystal-growth group in the Solid State Division at Oak Ridge National Laboratory. Slices of $\text{Mo}_{1-x}\text{Re}_x(110)$ were cut from the ingots and polished within 0.3° of the (110) orientation, as determined by Laue back-reflection. The samples were mounted individually on a high-precision ultrahigh vacuum goniometer and could be cooled with liquid nitrogen to < 130 K and also heated by electron bombardment to about 2100 K. The $\text{Mo}_{1-x}\text{Re}_x(110)$ samples were cleaned by several cycles of oxidation at 1500 K followed by sublimation of the oxide at 2000 K. For $x < 0.35$, $\text{Mo}_{1-x}\text{Re}_x$ is a random alloy where Mo and Re atoms are randomly distributed on a bcc lattice, and the composition of the top layer for (110) surfaces has been shown to be essentially the same as in the bulk.¹⁴ H-saturated $\text{Mo}_{1-x}\text{Re}_x(110)$ surfaces are prepared by exposure of the clean surface below 130 K to 50×10^{-6} Torr-sec of H_2 . Hydrogen molecules adsorb dissociatively, leaving a full monolayer of hydrogen atoms adsorbed in the quasi-threefold sites at saturation on all $\text{Mo}_{1-x}\text{Re}_x(110)$ surfaces at the sample temperatures where these experiments were performed.[14, 15]

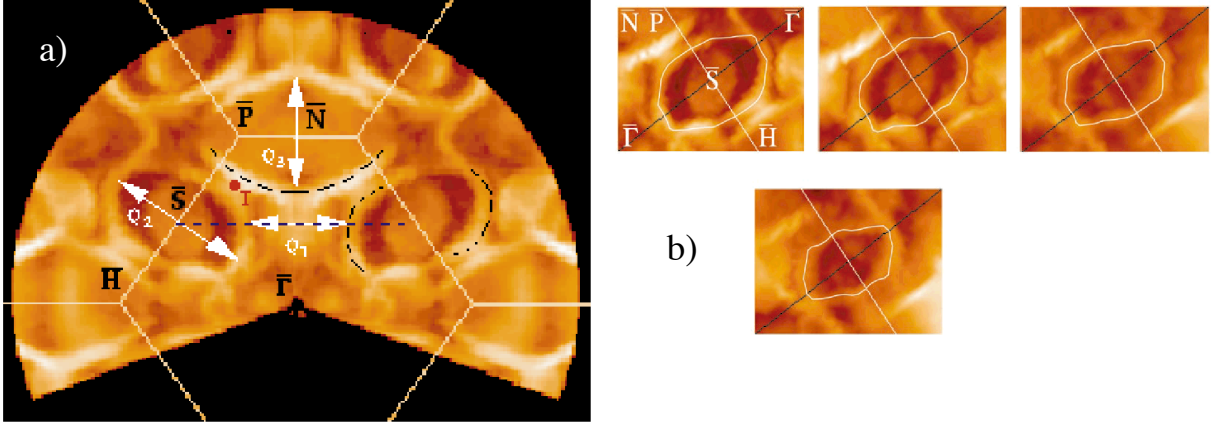


Fig. 1. (a) Experimentally determined Fermi photoelectron intensity for H-saturated Mo(110) with surface Brillouin zone indicated white lines. The white arrows Q_1 , and Q_2 correspond to the nesting vector in the $\bar{\Gamma}-\bar{\Gamma}$ and $\bar{\Gamma}-\bar{S}$ direction, respectively. The black lines are the theoretically predicted Surface states or resonances.⁴ (b) Fermi level intensity maps of the hole pocket surrounding the \bar{S} point for H-saturated $\text{Mo}_{1-x}\text{Re}_x(110)$, with $x = 0.00, 0.05, 0.15$, and 0.25 as indicated. Smooth curves are intended only to show that the shape of the pocket changes little with composition.

Fig. 1 (a) shows the measured photoemission intensity at the Fermi energy E_F on H-saturated Mo(110) as a function of momentum in the surface Brillouin zone. The brighter regions of the image result from a band crossing the Fermi level and thus indicate points on a 2D surface Fermi contour or a projected 3D Fermi surface. The lines marking the theoretically predicted surfaces states of Kohler, et al.⁴ have been included both to indicate the true surface states and also to illustrate the excellent agreement between experiment and theory. Fig. 1 (a) also illustrates with white arrows two important Fermi-spanning vectors Q_1 and Q_2 in the $\bar{\Gamma}-\bar{\Gamma}$ and $\bar{\Gamma}-\bar{S}$ directions, respectively. The magnitudes of these vectors (determined more precisely as discussed below) of 1.26 \AA^{-1} and 0.86 \AA^{-1} , respectively, agree quite well with the wave vectors of anomalies determined with HAS, $Q_2 = 1.23 \text{ \AA}^{-1}$ and $Q_1 = 0.89 \text{ \AA}^{-1}$.^{2,3} The recent ARPES measurements by Kröger et al.⁸ give $Q_2 = 1.19 \text{ \AA}^{-1}$ and $Q_1 = 0.85 \text{ \AA}^{-1}$ also agree with our results.

Fig. 1(b) displays Fermi level intensity maps of the roughly elliptical Fermi contour centered on the \bar{S} point of the SBZ as a function of Re concentration x . As indicated in Fig. 1(a), nesting of this hole pocket to its image across the $\bar{\Gamma}$ line and to itself across the \bar{S} point produces the observed anomalies at Q_1 and Q_2 , respectively. Therefore, changes in the size of this pocket as the alloy composition is varied will change the magnitude of the

nesting vectors. Given the approximate validity of the rigid band model in this system,^{12,13} the extra valence electron on rhenium will be donated to the host molybdenum band structure, thereby raising the Fermi level so as to maintain overall charge neutrality. We expect the hole pocket to decrease in size as x increases, and this is qualitatively observed. Moreover, the shape of the hole pocket remains very nearly constant as it shrinks. If we model this pocket as an ellipse, for example, the measured eccentricity ϵ increases only slightly, $0.76 \leq \epsilon \leq 0.78$, for $0.00 \leq x \leq 0.25$. We obtain a precise measure of the size of the two nesting vectors by plotting momentum distribution curves (MDC's) at the Fermi level along the relevant lines in the SBZ. An example is given in Fig. 2, which shows MDC's for the four surfaces along the $\bar{\Gamma}-\bar{S}-\bar{\Gamma}$ line. The decreasing magnitude of Q_2 is readily apparent, although the surface peak is masked on one side of \bar{S} by a nearby bulk feature.

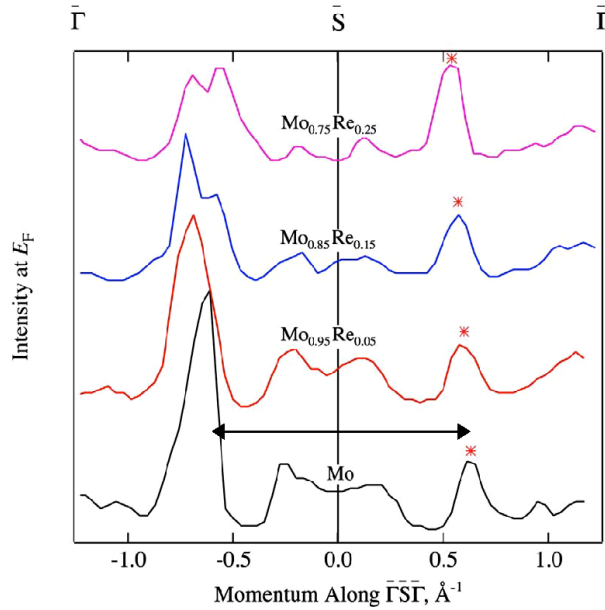


Fig. 2: Fermi level momentum distribution curves along the $\bar{\Gamma} \rightarrow \bar{S} \rightarrow \bar{\Gamma}$ direction for alloy surfaces in Fig. 1b). The nesting vectors are indicated, though a bulk feature interferes with the surface band on one side of \bar{S} .

The positions of the peaks in these MDC's provide a robust measure of the Fermi wave vectors and thereby also of the nesting vectors. The measured nesting vectors Q_1 and Q_2 are plotted in Fig. 3a) along with the measured positions of the anomalies from the HAS study.¹ The correspondence between the anomalies and the nesting vectors is seen to be

quite good, except for the highest concentration where the observed anomaly is quite broad and its position is difficult to measure with precision. We return to this point below. Note that the two nesting vectors evolve in different directions – Q_1 increases while Q_2 decreases. This provides further confirmation that the relevant nesting vectors span different ellipses in the case of Q_1 , but a single ellipse in the case of Q_2 . These results demonstrate that the electron-phonon coupling can be tuned by randomly alloying Mo and Re atoms, thereby altering the nesting vectors in the two-dimensional Fermi surface.

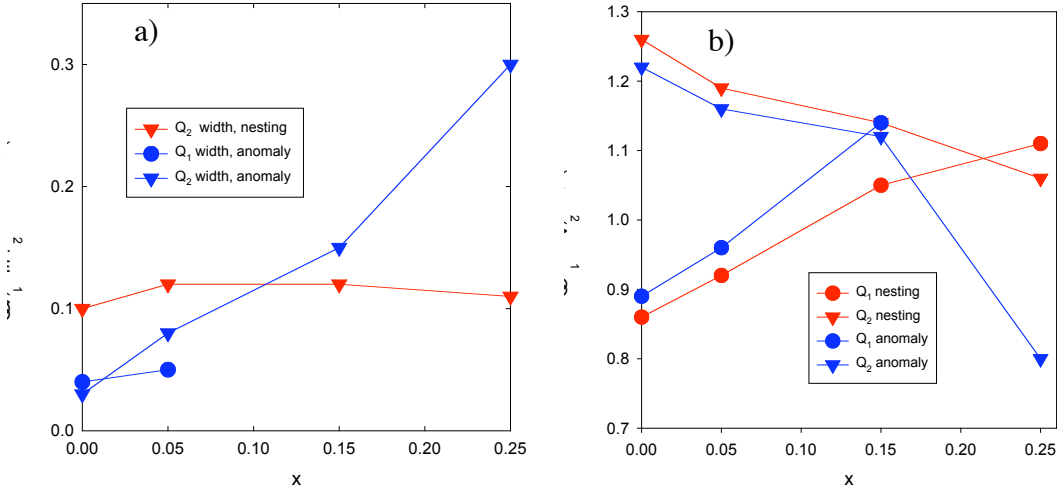


Fig. 3 a) Comparison of the recently reported positions of the surface phonon anomalies¹ along the $\bar{\Gamma}-\bar{\Gamma}$ and $\bar{\Gamma}-\bar{S}$ directions with our measured nesting vectors. b) A similar comparison of the reported width of the phonon anomalies and the width of surface peak from our momentum distribution curves.

Another notable feature of the HAS measurements is that the width of the observed phonon anomaly increases significantly with x , as plotted in Fig. 3b).¹ A possible cause of this broadening is that the electron bands are significantly k -broadened due to scattering by positional disorder in this random substitutional alloy, thereby broadening the nesting condition. However, the data in Fig. 2 do not support this notion, since the k -space width of the Fermi level crossings measured by our MDC's remains small and nearly constant. We have plotted the observed width of these crossings in Fig. 3b), and the mismatch between the width of the phonon anomaly and the width of the Fermi crossing is readily apparent. Indeed, most of the observed width is due to our experimental k -resolution, and the width of the peak in the MDC remains $< 0.05 \text{ \AA}^{-1}$. Recent coherent potential

approximation calculations confirm that this electronic broadening is much too small to explain the observed increase in width of the anomaly.^{12,13} The broadening of the phonon anomaly might also be caused by a changing degree of nesting as the rhenium concentration increases. The degree of nesting is inversely related to the difference in curvatures of the nested contours. Even though the nested contour has nearly constant shape, the curvature is indeed increasing as its size decreases, and this will naturally degrade the nesting condition. However, the curvature changes by only $\sim 20\%$ and is unlikely to produce the order of magnitude increase in the width of the anomaly observed in Fig. 3b).

We believe that the increasing width of the surface phonon anomaly is caused by scattering of the phonons off the positional disorder in the alloy. This scattering is apparently much larger than that of the electrons at the Fermi level, as evidenced by the data in Fig. 3b). This makes sense because the Re electron scattering potential can be effectively screened by the electron gas. This is, of course, an important ingredient of the success of the coherent potential approximation, which works quite well for electrons at the Fermi level in this alloy system. By contrast, the mass difference between molybdenum and rhenium cannot be screened, and the phonons will therefore be strongly scattered by substitutional rhenium atoms, leading to the observed broadening of the anomaly.

This conclusion has some bearing on how we understand the observed phonon anomalies for Mo(110)-(1 \times 1)H and W(110)-(1 \times 1)H. There actually are two anomalies,⁴ a deep one observed with HAS and discussed in this paper and a shallower one at the same wave vector seen by electron energy loss spectroscopy. It was argued⁴ that the former is mostly of electron-hole pair character, while the latter is mostly a surface vibrational mode. That analysis does not fit with our conclusion about the evolving width of the anomaly. If the deep anomaly is indeed electron-hole pair excitations, then the width should follow that of the underlying nested bands rather closely, contrary to our observations. We are forced to conclude that the distinction of electronic and vibronic anomalies may not be as clean as suggested previously.

Finally, we believe that our result is relevant to more complex alloy systems such as transition metal oxides, where doping is used to control and optimize electronic and

magnetic properties. Those properties are driven by manybody couplings between charge, spin, orbital, and lattice degrees of freedom. The randomness introduced by doping will broaden many of the relevant low-energy modes just as seen in this simpler metal alloy system. In the limit of very strong damping, these modes can become overdamped and localized. Nonetheless, the electronic degrees of freedom can and apparently do remain coherent with well-defined quasiparticles, as measured by photoemission,¹⁵ even though they are strongly coupled to the heavily damped degrees of freedom.

In summary, we demonstrated by Fermi mapping and band mapping that the nesting vectors in the two-dimensional Fermi surface can be tuned by the randomly alloying and as a result, electron-phonon coupling can be controlled. Moreover, useful insight into broadening mechanisms at surfaces can be gleaned from such measurements.

Acknowledgements

We would like to thank D.M. Zehner for supplying his crystal and the many useful discussions. This work was supported by NSF (EWP) DMR-9801830 and also supported by the Director, Office of Energy Research, Office of Basic Energy Sciences, Material Science Division, of the U.S. Department of Energy under Contract No. DE-AC03-76SF00098 and Grant No. DE-FG06-86ER45275. MO also acknowledges the Asahi Glass Foundation and the Kurata Memorial Science Foundation for financial support.

References

- ¹ M. Okada, B. Flach, E. Hulpke, et al., Surface Sci. **498**, L78 (2002).
- ² E. Hulpke and J. Lüdecke, Surface Sci. **272**, 289 (1992).
- ³ E. Hulpke and J. Lüdecke, Surface Sci. **287/288**, 837 (1993).
- ⁴ B. Kohler, P. Ruggerone, and M. Scheffler, Phys. Rev. B **56**, 13503 (1997).
- ⁵ B. Kohler, P. Ruggerone, S. Wilke, et al., Phys. Rev. Lett. **74**, 1387 (1995).
- ⁶ B. Kohler, P. Ruggerone, S. Wilke, et al., Zeitschrift f. Physikalische Chemie **197**, 193 (1996).
- ⁷ C. Bungaro, S. d. Gironcoli, and S. Baroni, Phys. Rev. Lett. **77**, 2491 (1996).
- ⁸ J. Kröger, T. Greber, and J. Osterwalder, Phys. Rev. B **61**, 14146 (2000).
- ⁹ E. Rotenberg and S. D. Kevan, Phys. Rev. Lett. **80**, 2905 (1998).
- ¹⁰ M. Hochstrasser, J. G. Tobin, E. Rotenberg, et al., Phys. Rev. Lett. **XX**, XXXX (2002).
- ¹¹ W. Kohn, Phys. Rev. Lett. **2**, 393 (1959).
- ¹² N. V. Skorodumova, S. I. Simak, I. A. Abrikosov, et al., Phys. Rev. B **57**, 14673 (1998).
- ¹³ M. Okada, E. Rotenberg, S. D. Kevan, et al., submitted to Phys. Rev. B.
- ¹⁴ L. Hammer, M. Kottcke, M. Taubmann, et al., Surface Sci. **431**, 220 (1999).
- ¹⁵ A. Damascelli, Z. Hussain, and Z.-X. Shen, Rev. Mod. Phys. **75**, 473 (2003).